full paper online (1)

Data · March 2016

CITATIONS
0

READS
87

8 authors, including:

T. M. W. J. Bandara
University of Peradeniya
51 PUBLICATIONS **725** CITATIONS
SEE PROFILE

Saumya Jayasundara
University of Manitoba
15 PUBLICATIONS **208** CITATIONS
SEE PROFILE

Lakshman Dissanayake
National Institute of Fundamental Studies - Sri Lanka
181 PUBLICATIONS **2,504** CITATIONS
SEE PROFILE

Maurizio Furlani
University of Gothenburg
43 PUBLICATIONS **478** CITATIONS
SEE PROFILE

J Appl Electrochem
DOI 10.1007/s10800-015-0788-1

RESEARCH ARTICLE

Efficiency of 10 % for quasi-solid state dye-sensitized solar cells under low light irradiance

T. M. W. J. Bandara · W. J. M. J. S. R. Jayasundara · H. D. N. S. Fernado · M. A. K. L. Dissanayake · L. A. A. De Silva · I. Albinsson · M. Furlani · B.-E. Mellander

Received: 11 October 2014 / Accepted: 28 January 2015

Abstract Polyacrylonitrile-based gel electrolytes were prepared using tetrapropylammonium iodide salt for dye-sensitized solar cells (DSSCs). The optimized gel electrolyte exhibited an ionic conductivity of 2.6 mS cm^{-1} at 25 °C and the DSSC fabricated with this gel electrolyte showed open-circuit voltage, short-circuit current density, fill factor, and efficiency of 0.71 V, 11.8 mA, 51, and 4.2 %, respectively, under one sun irradiation. The efficiency of the cell increases increased with decreasing solar irradiance achieving 10 % efficiency and 80 % fill factor at 3 mW cm^{-2} a low irradiance value of 3 mW cm^{-2}. Lower efficiencies at higher intensities were attributed to transport limitation of the redox mediators at high irradiation intensities. This work suggests that quasi-solid state DSSCs can reach efficiencies close to that of liquid electrolyte-based cells at low irradiance levels. The results open up new vistas on efficiency improvement in DSSCs by optical manipulation and control of DSSCs.

Keywords Dye-sensitized solar cells · Gel polymer electrolyte · Polyacrylonitrile · Light intensity · Low light irradiation · Efficiency enhancement

T. M. W. J. Bandara (✉) · H. D. N. S. Fernado
Department of Physics, Rajarata University of Sri Lanka, Mihintale, Sri Lanka
e-mail: awijendr@yahoo.com

T. M. W. J. Bandara · B.-E. Mellander
Department of Applied Physics, Chalmers University of Technology, Gothenburg, Sweden

W. J. M. J. S. R. Jayasundara · M. A. K. L. Dissanayake
Postgraduate Institute of Science, University of Peradeniya, Peradeniya, Sri Lanka

M. A. K. L. Dissanayake
Institute of Fundamental Studies, Hantana Road, Kandy, Sri Lanka

L. A. A. De Silva
Department of Physics, University of West Georgia, Carrollton, GA 30118, USA

I. Albinsson · M. Furlani
Department of Physics, University of Gothenburg, Gothenburg, Sweden

1 Introduction

During the last few decades, intense research efforts have been focused on developing more robust, practical, and economical solar cells in order to make devices that would supplement future energy needs. Since the first report on dye-sensitized solar cells (DSSCs) by O'Regan and Grätzel in 1991 [1], considerable research activities have been devoted to developing this type of solar cells as low-cost solar energy conversion devices with high efficiency. As a result of these efforts, many drawbacks associated with DSSCs have now been overcome and substantial progress has been made so that these cells have emerged as the third generation of practical solar cells [2].

DSSCs based on liquid electrolytes containing I^-/I_3^- or Co^{+2}/Co^{+3} redox mediators have been reported to have relatively high efficiencies of up to about 12 %. Many of them, however, contain electrolytes based on volatile solvents such as acetonitrile which limit the stability of the device [2–5]. In particular, the long-term performance or the stability of DSSCs is limited due to the leakage and volatilization of the organic solvent, which is inherited from the liquid electrolytes. In order to overcome these shortcomings, several attempts have been made on exploring alternative materials to replace the conventional

Published online: 04 February 2015

liquid electrolyte. For examples, the liquid electrolyte has been replaced by *p*-type semiconductors, organic hole conductors, and polymer gel electrolytes [6–10]. Out of these alternatives so far, the gel polymer electrolytes or quasi-solid-state electrolytes have emerged as one of the best substitutes [8–10]. Most of the gel electrolyte systems are non-volatile and have additional advantages such as improved nonflammability, diminished vapor pressure, and good adhesivity with the nanocrystalline semiconductor electrode [9, 10]. Further, they provide better leak-proof cell conditions and more importantly, the manufacturing is simplified because the electrolyte itself can act as a mechanical separator between the anode and the cathode. A major disadvantage of these gel electrolytes, however, is their relatively low ionic conductivity compared to that of liquid electrolytes. This results in generally lower performance for the gel electrolyte-based DSSCs than for the traditional liquid electrolyte-based devices [10].

Polyvinylidene fluoride (PVDF)-, polyacrylonitrile (PAN)-, and polyethylene oxide (PEO)-based gel electrolytes have been widely tested in laboratory scale DSSCs, but as expected the reported efficiencies are lower than those of cells with liquid electrolytes. At the same time, it has been shown that PAN and PVDF offer a better choice for gel electrolytes than other polymeric systems [11, 12]. Especially, polyacrylonitrile (PAN) has emerged as a reliable and non-volatile host polymer for DSSC electrolytes and an energy conversion efficiency of 7.27 % has been reported for these cells [9]. Thus, in this work, PAN has been chosen as the host polymer. It is difficult to compare reported efficiency values in the literature directly with the present work since some reported electrolytes contain more liquid components or highly volatile solvents. Further, tetrapropylammonium iodide (Pr_4NI) was taken as the iodide salt since it has been shown to give the highest performance out of the quaternary ammonium salts [8]. Ethylene carbonate (EC) and propylene carbonate (PC) co-solvents with high boiling points were chosen as the plasticizers for the PAN-based gel electrolyte system. In the present work, limited amounts of EC and PC (non-volatile solvents) were incorporated to the electrolyte to maintain better gel behavior. Rheological measurements of comparable PAN, EC, PC compositions (without salt) have not shown a gel–sol transition up to 75 °C [13]. In addition, it is reported that, when salts (tetrahexylammonium, MgI_2) were added, this (gel–sol) transition moves to higher temperatures [13]. Hence, the present electrolyte containing tetrapropylammonium iodide salt was also expected to maintain gel behavior at least up to 75 °C. However, a detailed study on sol–gel transformations of the electrolyte was not done since the major focus of the present work is to study the efficiency of the gel electrolyte-based DSSCs as a function of the intensity of incident light. Dye-sensitized solar cells, in general, have a lower efficiency compared to silicon *p-n* junction solar cells but under low light intensity and in diffused light, the efficiency increases for the dye-sensitized cells compared to their efficiency under full sunlight. However, to our knowledge there are no published reports on detailed studies on the performance of gel electrolyte-based DSSCs under varying light irradiation levels [14].

In laboratory tests, it is a common practice to use a one sun solar simulator (1,000 W m^{-2}) as the standard irradiance and 1.5 AM condition to characterize different types of solar cells. However, when the cell is used in real outdoor applications, it will not receive a constant irradiance of 1,000 W m^{-2}. Further, depending on the geographical location, the time of the day, and weather and climatic conditions, the solar irradiance varies and in general it is lower than 1,000 W m^{-2}. Therefore, it is very important to study the dependence of the solar cell performance in a wide range of irradiance levels prior to utilizing them in real-world applications. For instance, Tatsuo Toyoda et al. [15] clearly demonstrated that the one sun condition is not a decisive factor in evaluating the performance of solar cells. In their study, the energy conversion efficiency obtained by the certified measurement under one sun condition did not always coincide with the electricity-generated outdoors annually [15]. Further, the same authors reported that large-scale DSSC modules were made with 64 devices connected in series. The performance of the modular system was monitored for a half-year. Quite interestingly, this system showed the potential use of DSSCs for outdoor applications, since it demonstrated a 10–20 % higher electricity generation than that of conventional crystalline-Si modules. Thus, the study of DSSCs at low irradiance levels appears to be an important area in DSSC research. Therefore, in our present work, the performance of quasi-solid state, dye-sensitized solar cells was studied under different irradiation levels.

In addition, the modeling of DSSCs is important in order to understand the mechanism of charge transport in different components in the DSSC [16, 17]. It may also help understand the critical steps of the energy conversion process in order to design DSSCs with higher performance. A number of models and equivalent circuits for DSSCs can be found in the literature [3, 16, 17]. In the present work, we have used the method described by Guliani et al. [16] to understand the performance and characteristics of DSSCs through the model of series and shunt resistances. This equivalent circuit can reproduce the various cell performance parameters such as the open-circuit voltage (V_{oc}), short-circuit current (I_{sc}), maximum power point (P_m), and fill factor (*FF*). The photocurrent generated, I_{ph}, in Guilini's model represents the current produced when the photons are absorbed by the sensitizer and the subsequent

charge separation owing to the injection of the photogenerated electron into the conduction band of the semiconductor. The charge carrier recombination limits the collection efficiency of electrons in the external circuit. When the cell is in series with an external resistive load, i.e., when the current in the external circuit is limited, the recombination becomes more important and significantly reduces the cell performance. The kinetics of recombination is characterized by the electron lifetime, which has been observed to depend strongly on light intensity [18]. In this paper, the conductivity of the electrolyte and the characteristics of the device will also be discussed in detail.

2 Experimental

2.1 Materials

Polyacrylonitrile (PAN, M.W. 150,000), tetrapropylammonium iodide (Pr_4NI), iodine, ethylene carbonate (EC), and propylene carbonate (PC) all with purity greater than 98 % from Aldrich were used as starting materials. Prior to use, Pr_4NI and PAN were vacuum dried for 24 h at 150 and 50 °C, respectively. Conducting glass substrates (Fluorine-doped tin oxide (FTO) over-layer with sheet resistance of 7 Ω cm^{-2}), Pt-coated (mirror type) FTO, and sensitizing dye *cis*-diisothiocyanato-bis (2,2-bipyridyl-4,4-dicarboxylate) ruthenium(II) bis(tetrabutylammonium) (N719) were purchased from Solaronix SA. Nanocrystalline TiO_2 P25 and P90 were supplied by Degussa, Germany.

2.2 Electrolyte preparation

The gel electrolyte was prepared using PAN (1.0 g), EC (4.0 g), PC (4.0 g), Pr_4NI (0.6 g), and I_2 (0.05 g). EC, PC, and Pr_4NI were mixed in a closed glass bottle under continuous stirring at 50 °C for about 2 h. Then, PAN was added to the mixture, cooled to 40 °C, stirring for about 1 h. Finally, iodine was added to the mixture and heated to ~100 °C along with continuous stirring for a few more minutes. The resulting viscous solution was cooled down to room temperature, and the resulting gel was used for measurements and applications.

2.3 Device assembly

Two layers of TiO_2, one compact and the other porous, were deposited on the conducting glass substrate in order to prepare the photoanode. The compact layer was prepared using 0.5 g of, P90, TiO_2 powder. First, the TiO_2 powder was ground well for ~30 min with ~2 ml of HNO_3 (0.1 M) in an agate mortar. Then, the resulting slurry was spin coated on a well-cleaned FTO substrate using multispeed stages. The first stage was done at 1,000 rpm for 2 s and the second stage at 2,350 rpm for 60 s. During the spin-coating, a part of the glass plate was covered with adhesive tape to prevent coating TiO_2 on the part needed for electrical contacts. After air-drying for ~30 min, the TiO_2-coated substrate was sintered in air at 450 °C for ~30 min. Subsequently, the porous layer of TiO_2 was coated on the compact layer using P25 TiO_2 powder. For the preparation of this porous layer, 0.5 g of TiO_2 powder P25 was ground well for ~30 min with ~2 ml of HNO_3 (0.1 M) in an agate mortar. The resulting colloidal suspension was diluted to get a 5 % (w/w) mixture and subsequently, it was stirred overnight at 60 °C in order to obtain a 25 % (w/w) mixture. Then, two drops of Triton X 100 (surfactant) and ~0.1 g of MTO-Carbowax 1540 were added and mixed. The resulting colloidal suspension was coated using the doctor blade method followed by sintering in air at 450 °C for 30 min to obtain a mesoporous TiO_2 layer on top of the compact film. The total film thickness of TiO_2 was about 10 μm. The dye adsorption was carried out soaking the TiO_2-coated FTO plates in an ethanol solution of N 719 dye at ~60 °C and the keeping it for ~24 h at room temperature. The DSSCs were prepared by sandwiching a pre-heated thin layer (~0.1 mm) of electrolyte between the TiO_2 photoanode and the platinum-coated glass plate (mirror type).

2.4 Measurements

Complex impedance measurements were performed using a HP 4292A RF impedance analyzer in the 10 Hz–10 MHz frequency range to obtain the ionic conductivity of the electrolyte. For these measurements, the temperature of the sample was varied from 0 to 60 °C in 5 °C steps. Fabricated solar cells were illuminated under a LOT-Oriel GmbH solar simulator 1.5 AM, 1,000 Wm^{-2} (one sun). *I–V* characterization of the cells was obtained using a eDAQ Potentiostat and e-coder. In order to vary the irradiance of the simulated light gray metal reflective calibrated MELLES GRIOT filters were used. The area of the cell exposed to light was kept at 11 mm^2.

3 Results and discussion

3.1 Conductivity of the electrolyte

The polymer electrolytes containing PAN host polymer, plasticizing co-solvents EC and PC and Pr_4NI and I_2 and fabricated according to the procedure described in Sect. 2.2, exhibited gel nature and can be classified as quasi-solid electrolytes. The ionic conductivity (in logarithmic scale) of the electrolyte, obtained using complex impedance measurements, is shown in the inset in Fig. 1 as

a function of 1,000/T. The top x axis of the inset specifies the temperature in °C. The electrolyte has an ionic conductivity of 2.6 mS cm^{-1} at 25 °C and it increases to 4.8 mS cm^{-1} when heated to 60 °C. When the temperature is very low (~0 °C), the electrolyte still shows a conductivity of about 1.3 mS cm^{-1}.

The conductivity (σ) variation with temperature of the electrolyte was found to follow Vogel–Tammann–Fulcher (VTF) behavior. The data were fitted to the VTF equation;

$$\sigma = AT^{-1/2}\exp\left(-\frac{E_a}{k_B(T - T_g')}\right), \quad (1)$$

where σ, T, A, E_a, are the conductivity, the absolute temperature, a pre-exponential factor, the pseudo activation energy, respectively, and T_g' the reference temperature which is related to the equilibrium state glass transition temperature [19]. In this work, the measured glass transition temperature, T_g = 101.4 °C, was used as the reference temperature T_g' for fitting as reported by us for a comparable PAN-based electrolyte systems in an earlier report [8]. The rationality of employing T_g for T_g' is ratified by the good fitting for the measured temperature range, which is shown in Fig. 1. The standard deviation for the slope and intercept is as low as 1 %. The obtained values for E_a and A by fitting conductivity data to Eq. (1) are 32.5 meV and 92.7 S m^{-1} $K^{1/2}$, respectively.

The ionic conductivity (in logarithmic scale) of the electrolyte, obtained using complex impedance measurements, is shown in the inset in Fig. 1 as a function of 1,000/T. The top x axis of the inset specifies the temperature in °C. The electrolyte has an ionic conductivity of 2.6 mS cm^{-1} at 25 °C and it increases to 4.8 mS cm^{-1} when heated to 60 °C. When the temperature is very low (~0 °C), the electrolyte still shows a conductivity of about 1.3 mS cm^{-1}.

3.2 J–V characteristics

As discussed in Ref. [20], six separate, functionally active layers can be identified and described in a dye-sensitized solar cell in order to understand its performance. The roles played by each of these layers should be understood in terms of optics, electrochemistry, and electronics. The charge generation and transport are the principal factors governing the performance of a DSSC. Sunlight is absorbed by the dye and the photo-excited dye injects electrons into the conduction band of the TiO_2. Subsequently, the dye is rapidly regenerated by accepting an electron from the redox couple in the electrolyte. The injected electrons diffuse through the TiO_2 layer to reach the conducting FTO substrate and then travel through an external electric circuit (load) to the counter electrode, where they reduce the oxidized redox species (tri-iodide). Accordingly, the diffusion length of electrons, the electron injection efficiency, and the back electron transfer are the crucial factors governing the performance of a DSSC [21]. When the dye is regenerated at the dye/electrolyte interface by accepting electrons from iodide ions, tri-iodide ions are formed. The resulting tri-iodide ions diffuse to the Pt counter electrode where they are reduced to iodide. Thus, the effect due to the impedance caused by slow tri-iodide diffusion is rate determining for the solar cell performance. This effect of slow tri-iodide transport is more significant for quasi-solid polymer electrolytes than for liquid electrolytes owing to faster kinetics in liquid phases.

Figure 2 shows the current density versus cell potential (J–V) characteristic curves of the DSSCs fabricated with PAN/EC/PC:Pr_4NI gel polymer electrolyte for different

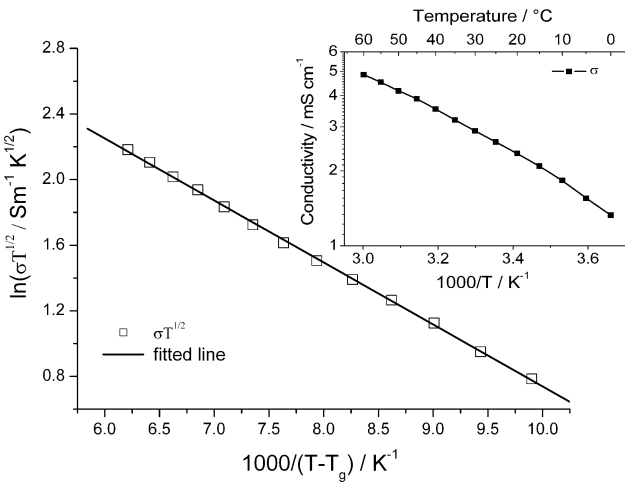

Fig. 1 Conductivity versus 1,000/T variation for PAN/EC/PC:Pr_4NI gel polymer electrolyte. T_g is the experimentally measured glass transition temperature of the gel electrolyte

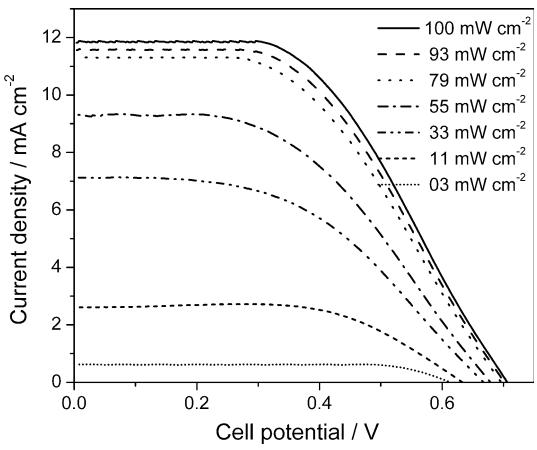

Fig. 2 Current density versus cell potential for quasi-solid state DSSCs with PAN/EC/PC:Pr_4NI electrolyte under irradiation with different light intensities

light intensities. The intensity of the irradiated light varied starting from (one sun) 100 mW cm^{-2} to very low 3 mW cm^{-2} using neutral density filters. The used intensity values are 100, 93, 79, 55, 33, 11, and 3 mW cm^{-2}. As the incident light intensity decreases, both the open-circuit voltage (V_{oc}) and the short-circuit current density (J_{sc}) decrease, as expected, due to the reduction of the density of photo-generated electrons. In general, the *J–V* behavior for a DSSC is given by [15].

$$J = J_{ph} - J_{\circ}\left(e^{\frac{e(V+R_sJ)}{nkT}} - 1\right) - \frac{V + R_sJ}{R_{sh}}, \quad (2)$$

where J_{ph} is the photocurrent density, J_0 the saturation current density, R_s the series resistance, R_{sh} the shunt resistance of the DSSC and, n an ideality factor, e the elementary electric charge, k the Boltzmann constant, and T the absolute temperature.

As seen in Fig. 2, the current density, *J,* of the DSSC decreases with decreasing intensity of light for the entire measured voltage range. This is primarily due to the decrease in net photocurrent generated, J_{ph}, which largely depends on the number of photons incident on the cell. Photocurrent density can also be given by $J_{ph} = J_{inj} - J_{sr}$, where J_{inj} is the electron injection (current resulting from dye oxidization) and J_{sr} is the surface recombination current [22]. The injected electrons can also undergo surface recombination with either the oxidized redox couple in the electrolyte or oxidized dye molecules. At high concentrations of I^- ions, the recombination currents can be neglected. However, when the tri-iodide concentration is high in the vicinity of the photoelectrode surface recombination is significant. J_{inj} is directly proportional to the incident photon flux [22], so the possible small variations of recombination and of light-harvesting efficiency with intensity change can also be neglected since the internal quantum efficiency of DSSCs containing N 719 dye has reached almost 100 % [23]. Moreover, the contributions from other effects such as transport limitations due to large variation of photocurrent with light intensity (photon flux) are dominant factors [18] in particular for quasi-solid DSSC.

3.3 Open-circuit voltage

The variation of V_{oc} against irradiance is shown in Fig. 3 and the inset shows the V_{oc} as a function of intensity in log scale. The V_{oc} of the cell goes down from 0.71 to 0.61 V when the intensity of light decreases from 100 to 3 mW cm^{-2}. The V_{oc} decreases more or less linearly with decreasing irradiance down to ~33 mW cm^{-2} while it falls more steeply for lower irradiance levels. Boschloo and Hagfeldt [24] have predicted a decrease of about 59 mV in V_{oc} for a one decade decrease of light intensity using their

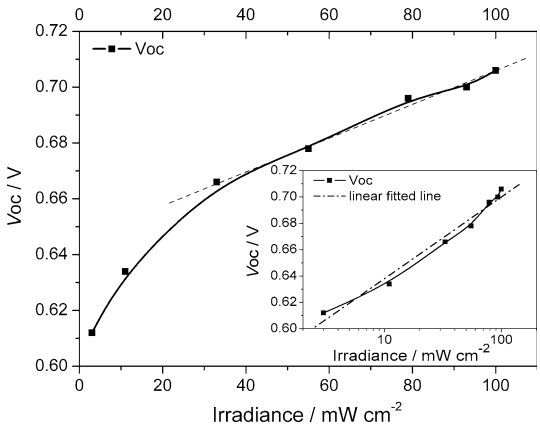

Fig. 3 Open-circuit voltage (V_{oc}) as a function of intensity of the incident light for the quasi-solid state DSSC with PAN/EC/PC:Pr_4NI electrolyte

equation for V_{oc}, however, their experimental results have shown larger values (~66 mV). Liu et al. also observed a similar average slope of the linear plots of about 64 mV per decade [25]. In the present study on quasi-solid state cells, a drop of about 70 mV has been observed when the light intensity is reduced by one decade, more explicitly from 100 to 11 mW cm^{-2}. The non-linear behavior of V_{oc} with intensity of light can be due to the non-linear reduction of the photocurrent due to transport limitations of the redox mediator in this quasi-solid state electrolyte.

The open-circuit voltage of a DSSC depends upon factors such as temperature, light intensity, electrode thickness, and transport limitations of the tri-iodide ions etc. [16]. When the light intensity varies, two competing factors control the V_{oc} in a DSSC. When the light intensity increases, the charge generation rate increases and consequently the chemical potential in the device gives rise to an increase in V_{oc}. On the other hand, an increased intensity reduces the lifetime of the charge leading to a decrease in chemical potential which results in a decrease in V_{oc}. However, the dominant factor among these two is the effect from charge generation [16] and thus V_{oc} increases with increasing intensity as shown in Fig. 3. Snaith et al. [26] have also observed that the intensity dependence of V_{oc} is more dependent on the charge generation rate than on the recombination rate constant, resulting in an increased chemical potential with increasing light intensity for solid state DSSCs. However, in their study monochromatic light with very low intensity (0.1–10 mW cm^{-2}) was used and the authors observed a linear relation of V_{oc} with intensity in logarithmic scale. This may be due to the narrow intensity range used since low photocurrents are essentially not affected by diffusion limitations of tri-iodide. In the present study, a non-linear behavior for the intensity dependence of V_{oc} is observed even in logarithmic scale (see the inset in Fig. 3). The average gradient over all

intensities are about 2.4 kT/e for this cell. However, at low intensities (<10 mW cm^{-2}), the gradient is about 1.5 kT/e.

The open-circuit voltage of the cell as a function of current density can generally be described by the following equation [24, 25]:

$$V_{oc} = \frac{kT}{e} \ln\left(\frac{J_{inj}}{k_{rec} n_{cond} [I_3^-]}\right), \qquad ((3))$$

where k_{rec} is the rate constant for tri-iodide reduction, and n_{cond} the conduction band electron density in the dark and $[I_3^-]$ the concentration of I_3^-. First-order recombination kinetics for both electrons and tri-iodide are assumed in the equation. Huang et al. [22] included an additional electron transfer coefficient in their expression. However, when we apply this equation for quasi-solid state electrolytes, a parameter to represent the poor mobility of tri-iodide should be taken into account, especially when the photo-generated current is high and the conductivity of the electrolyte is low this effect is more significant. The effect due the low conduction of the redox mediators can also be represented by the series resistance in the equivalent circuit [16]. Owing to the high conductivity in liquid electrolytes and to the low intensities used, a clear linear relationship (V_{oc} vs. log intensity) can be observed with data available from literature [18, 21, 26]. Conversely, when the V_{oc} variation is studied over a broad intensity range one could distinguish contributions from different intensity regions on DSSC performance [27]. Also, when the photo-generated current densities are high and the tri-iodide diffusion is inadequate, the effect from slow tri-iodide diffusion is visible [28, 29]. By studying the time dependence of the photocurrent with fixed incident power on the cell but decreasing the illuminated area (i.e., increasing the intensity), a faster initial increase of the photocurrent and a subsequent decrease of the steady-state value of the photocurrent have been observed [28, 29]. In that study, Trupke et al. clearly explained the suppression of photocurrent due to limitation of diffusion of the redox mediator. Thus, the observed linear drop of the V_{oc} at high intensities should be due to an increase of the tri-iodide concentration in the vicinity of the photo electrode due to the slow diffusion of tri-iodides in this quasi-solid state electrolyte. In this region, the current and voltage are controlled by the limitation of the diffusion of tri-iodides, thus possibly the series resistance [16] is dominated by impedance caused by slow tri-iodide diffusion.

3.4 Short-circuit current

The variation of J_{sc} with incident light intensity is shown in Fig. 4. The J_{sc} drops from 11.8 to 0.6 mA cm^{-2} with decreasing intensity of the light. The drop of J_{sc} is primarily due to the decrease of the number of photons incident on the cell which in turn decreases the photo-generated electrons that produces the photocurrent or charge generation. The other factors governing the J_{sc} is the amount of light trapping by the photo electrode which can be a function of light intensity, and the rate of recombination. DSSCs containing liquid electrolytes have shown a linear relationship between the photocurrent density and the irradiance levels as already mentioned [28]. However, a non-linear J_{sc} relation with light intensity as shown in Fig. 4 has earlier been observed for viscous electrolytes, where it has been attributed to transport limitations in the electrolyte [29]. One difference seen in the study by Sommeling et al. [28] is that monochromatic light with an intensity range 0–100 mW cm^{-2} has been used whereas in the present work white light is used in the same intensity range. However, the observed non-linearity in the present study can also be attributed to the mass transport limitations of the gel electrolyte used since the ion transport in viscous electrolytes and gel electrolytes are somewhat analogs, both characterized by slower ionic diffusion compared to that in low-viscosity liquids. The reasonably good J_{sc} value for quasi-solid DSSCs at low light intensities, 7.1 and 2.6 mA cm^{-2} at 33 and 11 mW cm^{-2} for example, is an important observation made in this study. The dashed line in Fig. 5 indicates the theoretically possible values of J_{sc} in absence of the recombination effect attributed by the tri-iodide high concentration. This kind of liner increase in J_{sc} has been observed for liquid electrolyte-based cells where diffusion of tri-iodide is high [29, 30].

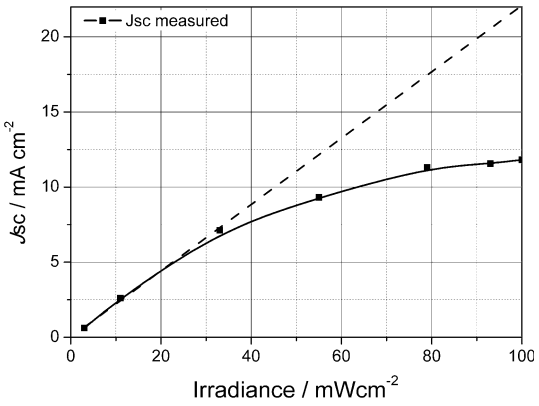

Fig. 4 Short-circuit photocurrent density (J_{sc}) as a function of the intensity of the incident light for the quasi-solid state DSSC with PAN/EC/PC:Pr_4NI electrolyte. *Dashed line* shows the expected J_{sc} if there is no redox mediator transport limitation

Table 1 shows the light intensity as a percentage of initial light intensity (100 mW cm^{-2} or one sun) and the current density of the cell as a percentage of initial current ($J_{sc,\ 1\ Sun}$) in order to understand the drop in J_{sc} with

decreasing light intensity. The increase of the efficiency and the decrease of V_{oc} with intensity drop as a percentages of their initial values (at one sun intensity) also are given in Table 1. Values in Table 1 clearly indicate that the drop of J_{sc} is much less than the drop of light intensity. For instance, when the intensity drops to 55 % relative to its initial value at one sun, J_{sc} drops only to 78.8 %, and when the intensity drops to 11 % the J_{sc} drops only to 22 %.

The incident photon-to-current conversion efficiency (IPCE) can be studied in order to understand the observed variation of J_{sc} with incident light intensity. Trupke et al. [28] have shown that with increasing intensity there is a slight increase of IPCE at very low light intensities followed by a drastic decrease of IPCE at very large intensities (photon density $>10^{18}$ cm^{-2} s^{-1}). The decrease of the IPCE at large light intensities is described to be due to the diffusion limitation of ions in the electrolyte inside the nanocrystalline electrode since large photocurrent densities lead to a significant depletion of the reducing ions at the location of the adsorbed dye molecules [28]. However, in their study a liquid electrolyte has been used while in the present work a quasi-solid electrolyte is used. Thus, the major reason for reduced efficiencies at high intensities can be attributed to diffusion limitations of the quasi-solid electrolytes used.

3.5 Open-circuit voltage versus short-circuit current

In order to analyze the current density in a DSSC by analyzing internal resistance elements Han et al. [3] have used the circuit diagram shown in Fig. 5. The series resistance corresponds to the resistance of the Pt counter electrode, R_1, to the Nernstian diffusion in the electrolyte, R_3, and to the sheet resistance of the transparent conductive substrate R_h. The charge transportation at the TiO_2/dye/electrolyte interface was found to act like the resistance of a diode, R_2, since it is dependent on the applied bias voltage [3].

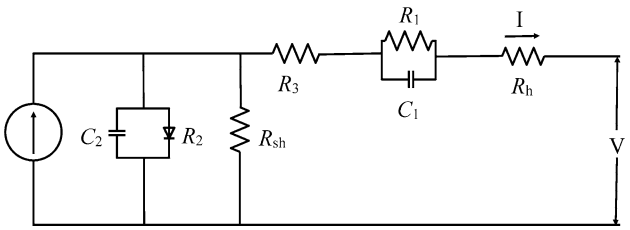

Fig. 5 Schematic diagram of the equivalent circuit for a DSSC as illustrated in Ref. [2]

The interrelationship between the photocurrent density and open-circuit voltage of the cell can generally be described by [25];

$$V_{oc} = \frac{nkT}{e} \ln\left(\frac{J_{ph}}{J_{\circ}}\right). \quad (4)$$

Different DSSCs have shown different values for the ideality factor, n, for instance 1.08, 1.4, 2.1, and 2.5 [15, 21, 24]. However, in the present study a non-linear behavior was observed for the open-circuit voltage (V_{oc}) as a function of short-circuit photocurrent density (J_{sc}) in a logarithmic scale (not shown). However, at low light intensities the value of the ideally factor is about 1.5 and it increases gradually with increasing light intensity.

3.6 Fill factor

The variation of the fill factor (*ff*) and voltage at maximum power output (V_{opt}) of the cell with the incident light intensity is shown in Fig. 6. According to Fig. 6, it is noteworthy that the variation of *ff* with intensity has shown a similar trend as that of the V_{opt}. For higher intensities of light, quite low fill factors of about 47–50 % are observed, but for low light intensities they increase up to 80 %. Generally, under low light intensity, the fill factor of DSSCs is improved because of low photocurrent (i.e., low series resistance since the transport limitation of tri-iodide has not yet been reached), resulting in improved cell performance [31]. In DSSCs low shunt resistance provides an alternative path for light-generated current leading to lower power output which subsequently decreases the fill factor. However, the series resistance should be as low as possible for an improved *ff*.

The essentially linear decrease of the fill factor with decreasing light intensity down to 30 mW cm^{-1} observed

Table 1 The light intensity as a percentage of initial light intensity (100 mW cm^{-2} or one sun) and respective variation of drop of J_{sc}, V_{oc} and efficiency as percentage of values at 100 mW cm^{-2}

(Intensity/one sun)/%	($J_{sc}/J_{sc,\ one\ sun}$)/%	($V_{oc}/V_{oc,\ one\ sun}$)/%	$\eta/\eta_{one\ sun}$/%
3.0	5.2	86.7	236.4
11.0	22.1	89.8	218.3
33.0	60.2	94.3	163.1
55.0	78.8	96.0	128.7
79.0	95.6	98.6	114.5
93.0	97.8	99.2	102.6
100.0	100.0	100.0	100.1

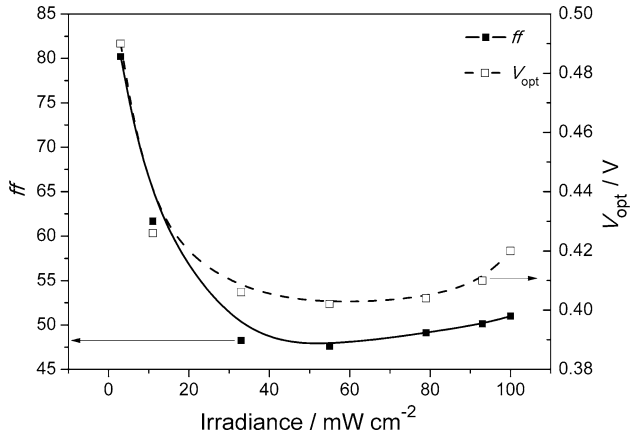

Fig. 6 The fill factor (*ff*) and the voltage at maximum power output (V_{opt}) as a function of intensity of the light for the quasi-solid state DSSC with the PAN/EC/PC:Pr_4NI electrolyte

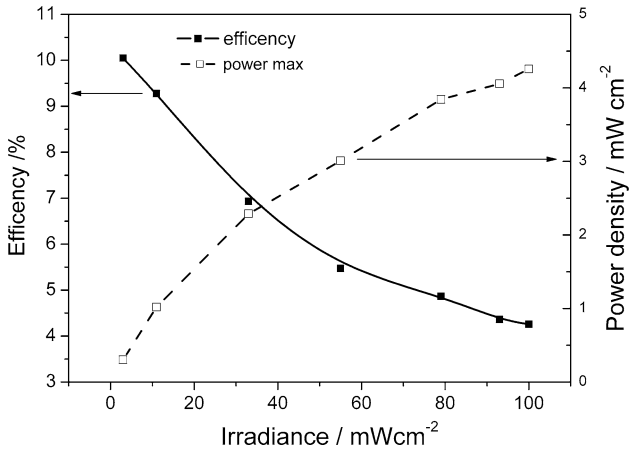

Fig. 7 The efficiency and maximum power output of the quasi-solid state DSSC with the PAN/EC/PC:Pr_4NI electrolyte as a function of intensity of the light

in this work can be attributed to effects related to shunt resistance as observed effects from charge recombination. The drastic increase of the fill factor in the low-intensity region can be due to a lowering of the series resistance for low currents which can be due to less severe diffusion limitations of tri-iodides as explained above. The fill factor is, in this case is high and it is, actually comparable to or better than that of DSSCs containing liquid electrolytes. At 3 mW cm^{-2} intensity, the fill factor is about 80 %. In literature, similar effect has been observed by Tennakone et al. for another comparable quasi-solid state DSSC [32]. They observed a fill factor increase from 59 to 72 % for an intensity drop of one decade.

3.7 Efficiency and power

The efficiency and the maximum power output of the cell as a function of the incident light intensity are shown in Fig. 7. For higher intensities of light, lower efficiencies are observed but when the light intensity decreases, the cell efficiency exhibits an increasing trend. For instance, when the irradiance is 3 mW cm^{-2}, the cell has shown 10.1 % efficiency. To our knowledge, this is the highest efficiency reported for a quasi-solid state DSSC at any intensity. A comparable system, but with SnO_2/ZnO photo electrode and PAN-based gel electrolyte with CsI salt, have observed efficiency increase from 4.1 to 9.0 % when the intensity decreases from 100 to 10 mW cm^{-2} (or 1,000–100 W m^{-2}) [31]. As a result of the increasing trend of the efficiency with decreasing light intensity, the cell has a power density of about 1 mWcm^{-2} for the light intensity of 11 mW cm^{-2}.

The reported best efficiency of liquid electrolyte-containing DSSCs is about 11–12 % with the redox couple I^-/I_3^- [2, 5] and 12–13 % with Co^{+2}/Co^{+3} [4]. Attempts were made to fabricate quasi-solid state DSSCs with Co^{+2}/Co^{+3} redox couple with polymer and plasticizers used in this study but these were not successful due to poor ionic conductivity. However, with I^-/I_3^- redox couple DSSCs could be fabricated with reasonable efficiency at one sun irradiance due to good iodide ion conductivity. However, neither mixed salts (for example, LiI is not incorporated) nor additives like 4-*tert*-butylpyridine were used to improve efficiency, as is reported in high-efficient DSSCs [1–3, 5, 14]. Finally, we can conclude that the performance of quasi-solid state DSSCs is very close to that of cells containing liquid-type electrolytes at low light intensities since at low light intensities the photocurrent is not suppressed by transport limitations of tri-iodides.

4 Conclusions

The gel polymer electrolyte complex PAN/EC/PC:Pr_4NI has shown ionic conductivities of 2.6 mS cm^{-1} at 25 °C and 4.8 mS cm^{-1} at 60 °C. When this electrolyte is used in a quasi-solid-state DSSC, V_{oc}, J_{sc}, *ff*, and efficiency values are 0.71 V, 11.8 mA, 51, and 4.2 %, respectively, at one sun (100 mW cm^{-2}) illumination. Irradiation dependence of J_{sc} shows that the drop in J_{sc} is quite slower than that of the light intensity. For instance, when the light intensity drops to 55 % and to 11 %, the J_{sc} drops only to 78.8 and to 22 %, respectively.

The important research finding of this work is that the fill factor and the efficiency of the cells increase with decreasing irradiance reaching 10 % efficiency and 80 % fill factor at low irradiance levels. This is the highest efficiency reported for a quasi-solid state DSSC at any intensity to our best knowledge. The efficiency of the cell has improved by

236 % for the intensity 3 mW cm^{-2} compared to intensity at 100 mW cm^{-2} (one sun). This effect was attributed to non-suppression of photocurrent due to low currents at low intensities by diffusion limitations of the redox mediator. The present work shows that the performance of quasi-solid state DSSCs is very close to that of liquid electrolyte-based DSSCs at low light intensities and that a limiting factor at higher light intensities is the low diffusion coefficient of the tri-iodide species.

This work also reveals not only the advantage of using dye-sensitized solar cells under low light intensities but also opens up the door for increasing the efficiencies of such cells by means of selective optics.

Acknowledgments The authors wish to thank the National Research Council (NRC) of Sri Lanka (Grant 11-196) and the Swedish Research Council (SRC) for financial support.

References

1. Regan BO', Grätzel M (1991) A low-cost, high-efficiency solar cell based on dye-sensitized colloidal TiO_2 films. Nature 353: 737–740
2. Hagfeldt A, Boschloo G, Sun L, Kloo L, Pettersson H (2010) Dye-sensitized solar cells. Chem Rev 110:6595–6663
3. Han L, Koide N, Chiba Y, Islam A, Komiya R, Fuke N, Fukui A, Yamanaka R (2005) Improvement of efficiency of dye-sensitized solar cells by reduction of internal resistance. Appl Phys Lett 86:213501
4. Yella A, Lee HW, Tsao HN, Yi C, Chandiran AK, Nazeeruddin MK, Diau EWG, Yeh CY, Zakeeruddin SM, Grätzel M (2011) Porphyrin-sensitized solar cells with cobalt (II/III)-based redox electrolyte exceed 12 percent efficiency. Science 334(6056): 629–634
5. Chiba Y, Islam A, Watanabe Y, Komiya R, Koide N, Han L (2006) Dye-sensitized solar cells with conversion efficiency of 11.1%. Jpn J Appl Phys 45(25):L638–L640
6. Leijtens T, Ding I-K, Giovenzana T, Bloking JT, McGehee MD, Sellinger A (2012) Hole transport materials with low glass transition temperatures and high solubility for application in solid-state dye-sensitized solar cells. ACS Nano 6(2):1455–1462
7. Xu C, Wu J, Desai UV, Gao D (2012) High-efficiency solid-state dye-sensitized solar cells based on TiO_2-coated ZnO nanowire arrays. Nano Lett 12(5):2420–2424
8. Bandara TMWJ, Jayasundara WJMJR, Dissanayake MAKL, Furlani M, Albinsson I, Mellander B-E (2013) Effect of cation size on the performance of dye sensitized nanocrystalline TiO_2 solar cells based on quasi-solid state PAN electrolytes containing quaternary ammonium iodides. Electrochim Acta 109:609–616
9. Ileperuma OA, Kumara GRA, Yang H-S, Murakami K (2011) J Photochem Photobiol A 217:308–312
10. Bella F, Bongiovanni R (2013) Photoinduced polymerization: an innovative, powerful and environmentally friendly technique for the preparation of polymer electrolytes for dye-sensitized solar cells. J Photochem Photobiol C 16:1–21
11. Lee K-M, Suryanarayanan V, Ho K-C (2009) High efficiency quasi-solid-state dye-sensitized solar cell based on polyvinylidene fluoride-co-hexafluoro propylene containing propylene carbonate and acetonitrile as plasticizers. J Photochem Photobiol A 207:224–230
12. Priya ARS, Subramania A, Jung Y-S, Kim K-J (2008) High-performance quasi-solid-state dye-sensitized solar cell based on an electrospun PVdF−HFP membrane electrolyte. Langmuir 24(17):9816–9819
13. Dinteheva NT, Furlani M, Jayasundara WJMJSR, Bandara TMWJ, Mellander B-E, La Mantia FP (2013) Rheological behavior of PAN based electrolytic gel containing tetrahexylammonium and magnesium iodide for photoelectrochemical applications. J Rheol Acta 52:881–889
14. Bandara TMWJ, Jayasundara WJMJSR, Fernado HDNS, Dissanayake MAKL, De Silva LAA, Fernando PSL, Furlani M, Mellander B-E (2014) Efficiency enhancement of dye-sensitized solar cells with PAN:CsI:LiI quasi-solid state (gel) electrolytes. J Appl Electrochem 44:917–926
15. Toyoda T, Sano T, Nakajima J, Doi S, Fukumoto S, Ito A, Tohyama T, Yoshida M, Kanagawa T, Motohiro T, Shiga T, Higuchi K, Tanaka H, Takeda Y, Fukano T, Katoh N, Takeichi A, Takeichi K, Shiozawa M (2004) Outdoor performance of large scale DSC modules. J Photochem Photobiol 164:203–207
16. Guliani R, Jain Kapoor A (2012) Exact analytical analysis of dye-sensitized solar cell: improved method and comparative study. J Open Renew Energy 5:49–60
17. Bay L, West K (2005) An equivalent circuit approach to the modelling of the dynamics of dye sensitized solar cells. Sol Energy Mater Sol Cell 87:613–628
18. Anta JA, Casanueva F, Oskam G (2006) A numerical model for charge transport and recombination in dye-sensitized solar cells. J Phys Chem B 110:5372–5378
19. Wang Y-J, Pan Y, Wang L, Pang M-J, Chen L (2006) Characterization of $(PEO)LiClO_4$-$Li1.3Al0.3Ti1.7(PO_4)_3$ composite polymer electrolytes with different molecular weights of PEO. J Appl Polym Sci 102:4269–4275
20. Wenger S, Schmid M, Rothenberger G, Gentsch A, Gratzel M, Schumacher JO (2011) Coupled optical and electronic modeling of dye-sensitized solar cells for steady-state parameter extraction. J Phys Chem C 115:10218–10229
21. Peter LM, Wijayantha KGU (1999) Intensity dependence of the electron diffusion length in dye-sensitised nanocrystalline TiO_2 photovoltaic cells. Electrochem Commun 1:576–580
22. Huang SY, Schlichthor G, Nozik AJ, Gratzel M, Frank AJ (1997) Charge recombination in dye-sensitized nanocrystalline TiO_2 solar cells. J Phys Chem B 101:2576–2582
23. Park N-G (2010) Methods to improve light harvesting efficiency in dye-sensitized solar cells. J Electrochem Sci Technol 1(2):69–74
24. Boschloo G, Hagfeldt A (2009) Characteristics of the iodide/triiodide redox mediator in dye-sensitized solar cells. Acc Chem Res 42–11:1819–1826
25. Liu Y, Hagfeldt A, Xiao X-R, Lindquist S-E (1998) Investigation of influence of redox species on the interfacial energetics of a dye-sensitized nanoporous TiO_2 solar cell. Sol Energy Mater Sol Cell 55:267–281
26. Snaith HJ, Schmidt-Mende L, Grätzel M, Chiesa M (2006) Light intensity, temperature, and thickness dependence of the open-circuit voltage in solid-state dye-sensitized solar cells. Phys Rev B 74:045306
27. Salvador P, Hidalgo MG, Zaban A, Bisquert J (2005) Illumination intensity dependence of the photovoltage in nanostructured TiO_2 dye-sensitized solar cells. J Phys Chem B 109:15915–15926
28. Trupke T, Wurfel P, Uhlendorf I (2000) Dependence of the photocurrent conversion efficiency of dye-sensitized solar cells on the incident light intensity. J Phys Chem B 104:11484–11488
29. Sommeling PM, Rieffe HC, van Roosmalen JAM, Schönecker A, Kroon JM, Wienke JA, Hinsch A (2000) Spectral response and IV-characterization of dye-sensitized nanocrystalline TiO_2 solar cells. Sol Energy Mater Sol Cell 62:399–410

30. Colodrero S, Calvo ME, Miguez H (2010) In: Rugescu RD (ed) Photon management in dye sensitized solar cells in solar energy. Intech, Croatia
31. Hara K, Arakawa H (2003) In: Luque A, Hegedus S (eds) Handbook of photovoltaic science and engineering. Wiley Ltd, Hoboken
32. Tennakone K, Senadeera GKR, Perera VPS, Kottegoda IRM, Silva LAAD (1999) Dye-sensitized photoelectrochemical cells based on porous SnO_2/ZnO composite and TiO_2 films with a polymer electrolyte. Chem Mater 11:2474